2018 ASEE Mid-Atlantic Section Spring Conference: Washington, District of Columbia Apr 6

Controller Design for Mechatronic Rotary Inverted Pendulum (Part 1 and Part 2)

Dr. Wangling Yu, Purdue University Northwest (Merged with Calumet)

Dr. Wangling Yu is an assistant professor in the Electrical & Computer Engineering Technology Department of the Purdue University Northwest. He was a test engineer over 15 years, providing technical leadership in the certification, testing and evaluation of custom integrated security systems. He received his PhD degree in Electrical Engineering from the City University of New York in 1992, specializing in control theory and electronic technology.

Analog Controller Design for Mechatronic Rotary Inverted Pendulum (Part 1)

Wangling Yu[1] and Hanlin Chen[2]

1 College of Technology, Purdue University Northwest, Westville, IN 46391
2 Polytechnic Institute, Purdue University, West Lafayette, IN 47907

Abstract

The mechatronic rotary inverted pendulum is a multidisciplinary multivariable control framework. To this fourth order dynamic system, this paper will involve the modeling, analysis, and analog controller design. The control approach and its effect are verified via numerical simulation results. These results can be generalized in the applications of various nonlinear systems' control design.

Keywords

Pole placement, rotary inverted pendulum, mechatronics

Introduction

The mechatronic rotary inverted pendulum, which is a typical fourth order dynamic system, is often used as a multidisciplinary multivariable test bed for many engineering controls. Evolution of control theory would lead to the research advances in technical development, the theory and methods for the designing of controller, and finally, real-time implementation of the controller designed. The rotary inverted pendulum is a highly unstable system with multi-input and multi-output feature.[1-2] The application of the rotary inverted pendulum are various, such as two-wheel robot[3], ball-on-plate system design[4], and it can be modified into models like two-pendulum system[5], and Furuta pendulum model[6]. It's dynamic properties can be applicable in applications like earthquake visualization.[7] It is noticeable that numerous methods had been applied to the rotary inverted pendulum system, the typical ones are PID controllers[8-9], PI controllers[10-11], Fuzzy control[12-14], LQR stabilization method[15], fractional order method[16], other control method which involves the computer engineering include methods like evolutionary algorithm[17], genetic algorithm, PSO-based controller design method[18], real-time optimal controller design[19]. Tuning process seemed to be a big problem for PID controllers when they are designed for rotary inverted pendulum[11], especially when models with different numerical descriptions applied, and they seemed to have a comparatively small margin comparing to other methods.[20] In this paper, with the stability and observability analysis of the linearized fourth order dynamic system, different responses of the system with various controllers implemented are investigated.

Modeling of Rotary Inverted Pendulum

The rotary inverted pendulum problem is deemed as a kind of challenge within the area of control system, [21-22] i.e., the mathematical modeling involves in nonlinearities, yet once it's linearized, it's

both uncontrollable and unobservable. [23] In the figure shown, the swing up phase is not included in the work scope. It is assumed that the rotary inverted pendulum system starts at its upright position with the initial conditions to be zero. [24] Euler-Lagrange Equation is employed to derive the system's dynamics, and the Lagrange function L is first constructed. [25]

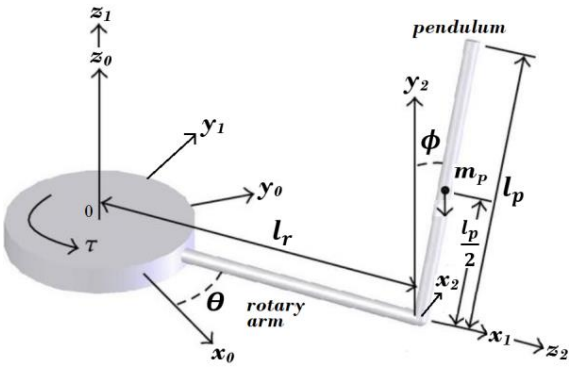

Figure 1. Rotary inverted pendulum and its coordinate systems

The Lagrange function L is defined as the difference of the kinetic energy and potential energy, and the equations describing these two energies respectively are expressed in terms of the variables in the specified coordinate systems as shown in Figure 1:

$$L = \left(\frac{1}{2}J_r + \frac{1}{2}m_p l_r^2\right)\dot{\theta}^2 - \frac{1}{2}m_p l_r l_p \dot{\theta}\dot{\phi}cos\phi + \left(\frac{1}{8}m_p l_p^2 + \frac{1}{2}J_p\right)\dot{\phi}^2 - \frac{1}{2}m_p l_p g cos\phi \quad (1)$$

After obtaining the Lagrange function for the system, from the Euler-Lagrange equation, the equations of motions for the rotary inverted pendulum can be derived:

$$\frac{d}{dt}\left(\frac{\partial L}{\partial \dot{q}}\right) - \frac{\partial L}{\partial q} + \frac{\partial E_d}{\partial \dot{q}} = F_q \quad (2)$$

where $q = [\theta, \phi]$, 2 degrees of freedom. F_q in equation (2) is generalized force. E_d is dissipated energy by frictions, such as viscosity and Coulomb friction. In this model, $E_d = 0$ is assumed. Euler-Lagrange Equation with respect to $\theta(t)$ leads to:

$$\left(J_r + m_p l_r^2\right)\ddot{\theta} - \frac{1}{2}m_p l_r l_p \ddot{\phi}cos\phi + \frac{1}{2}m_p l_r l_p \dot{\phi}^2 sin\phi = \tau \quad (3)$$

Euler-Lagrange Equation with respect to ϕ leads to

$$\left(J_p + \frac{1}{4}m_p l_p^2\right)\ddot{\phi} - \frac{1}{2}m_p l_r l_p \ddot{\theta}cos\phi - \frac{1}{2}m_p l_r l_p \dot{\theta}\dot{\phi}sin\phi = 0 \quad (4)$$

The system dynamic model is composed of equations (3) and (4). The linearized equations of motions are shown as below:

$$\left(J_r + m_p l_r^2\right)\ddot{\theta} - \frac{1}{2}m_p l_r l_p \ddot{\phi} = \tau \quad (5)$$

$$\left(J_p + \frac{1}{4}m_p l_p^2\right)\ddot{\phi} - \frac{1}{2}m_p l_r l_p \ddot{\theta} - \frac{1}{2}m_p g l_p \theta = 0 \quad (6)$$

where τ is the output torque of the DC motor, and

$$J_p = \frac{1}{12} m_p l_p^2, \quad J_r = \frac{1}{3} m_r l_r^2$$

For electrical DC motor, there exist the following relationship:

$$\tau = \frac{k_T (V_m - K_m \dot{\theta})}{R_m} \tag{7}$$

where K_T is the torque constant of the motor, and K_m is the EMF constant of the motor, V_m is the input voltage of the motor, and R_m is the armature resistance of the motor.

State Space Presentation of Rotary Inverted Pendulum System

Denoting

$$\begin{cases} c_1 = J_r + m_p l_r^2 \\ c_2 = -\frac{1}{2} m_p l_r l_p \\ c_3 = \frac{1}{4} m_p l_p^2 + J_p \\ c_4 = -\frac{1}{2} mpl_r l_p \\ c_5 = -\frac{1}{2} m_p g l_p \end{cases}$$

The state-space representation of the model can be written as:

$$\begin{bmatrix} \dot{\theta} \\ \ddot{\theta} \\ \dot{\phi} \\ \ddot{\phi} \end{bmatrix} = \begin{bmatrix} 0 & 1 & 0 & 0 \\ 0 & \frac{(c_3 * K_T * K_m)}{(R_m * (c_1 * c_3 - c_2 * c_4)} & \frac{c_2 * c_5}{c_1 * c_3 - c_2 * c_4} & 0 \\ 0 & 0 & 0 & 1 \\ 0 & \frac{c_4 * K_T * K_m}{R_m * (c_1 * c_3 - c_2 * c_4)} & -\frac{c_5}{c_3} & 0 \end{bmatrix} \begin{bmatrix} \theta \\ \dot{x}\theta \\ \phi \\ \dot{\phi} \end{bmatrix} + \begin{bmatrix} 0 \\ \frac{c_3 * K_T}{R_m * (c_1 * c_3 - c_2 * c_4)} \\ 0 \\ -\frac{c_4 * K_T}{R_m * (c_1 * c_3 - c_2 * c_4)} \end{bmatrix} u \tag{8a}$$

$$\begin{bmatrix} \dot{\theta} \\ \ddot{\theta} \\ \dot{\phi} \\ \ddot{\phi} \end{bmatrix} = A \begin{bmatrix} \theta \\ \dot{\theta} \\ \phi \\ \dot{\phi} \end{bmatrix} + Bu \tag{8b}$$

$$y = \begin{bmatrix} 1 & 0 & 0 & 0 \\ 0 & 0 & 1 & 0 \end{bmatrix} \begin{bmatrix} \theta \\ \dot{\theta} \\ \phi \\ \dot{\phi} \end{bmatrix} + \begin{bmatrix} 0 \\ 0 \end{bmatrix} u \tag{9}$$

Given a group of parameters, matrix A can be SVD decomposed:

$$A = U * \Sigma * V$$

U and V are unitary matrices as shown as below:

$$U = \begin{bmatrix} -0.001 & 0.1578 & 0 & 0.9875 \\ -0.6865 & 0.7180 & 0 & -0.1148 \\ 0 & 0 & -1 & 0 \\ -0.7271 & -0.6779 & 0 & 0.1082 \end{bmatrix}, \quad V = \begin{bmatrix} 0 & 0 & 0 & 1 \\ -0.0108 & 0.9999 & 0 & 0 \\ -0.9999 & -0.0108 & 0 & 0 \\ 0 & 0 & -1.0000 & 0 \end{bmatrix}$$

Matrix Σ is a diagonal matrix with eigenvalues of 1.0000, 6.3372, and 101.1267. By multiplying the first eigenvalue of Σ and U and V matrices, the following equation is obtained:

$$\dot{\theta} = U_{1,:} * \sigma_1 * V_{:,1} * \theta + B_1 u$$

where σ_1 is the first eigenvalue of matrix Σ, and $U_{1,:}$ represents the first row of the matrix U, $V_{:,1,}$ represents the first column of the matrix V. Similarly, other relations for the decoupled system can be presented as:

$$\ddot{\theta} = U_{2,:} * \sigma_2 * V_{:,2} * \dot{\theta} + B_2 u$$
$$\dot{\phi} = U_{3,:} * \sigma_3 * V_{:,3} * \phi + B_3 u$$
$$\ddot{\phi} = U_{4,:} * \sigma_{14} * V_{:,4} * \dot{\phi} + B_4 u$$

Stability, Sensitivity and Robustness, Controllability and Observability Analysis

In this section, the stability of the origianl system using methods like zero-poles methods, Nyquist diagram, root locus and other methods will be investigated. To check the over-all stability of the rotary inverted system, the zero-poles graph of the system is produced. The plot revealed that two poles in the right plane and none-zeros in the right plane, which indicates that the original system is not stable. (see Figure 2a) The system's instability can also be observed by other methods like Nyquist Diagram (Figure 2b) and Bode diagram (Figure 3).

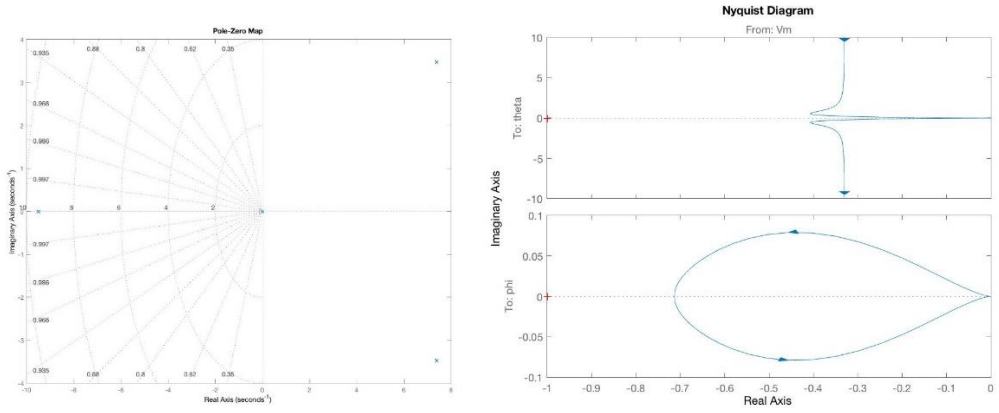

(a) (b)

Figure 2. Pole-zero map and Nyquist diagram of rotary inverted pendulum system

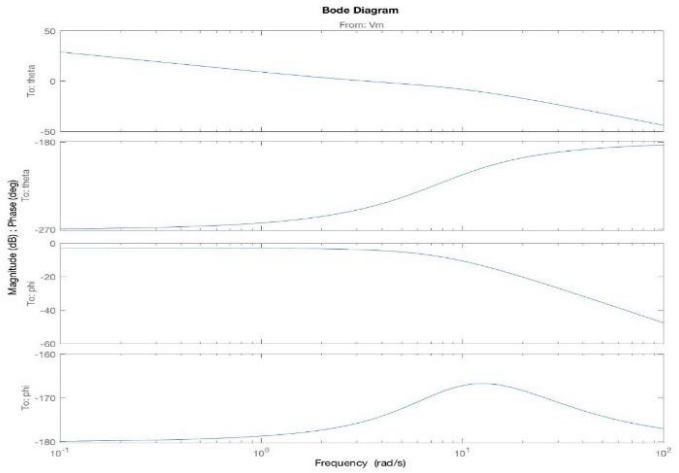

Figure 3. Bode diagram of rotary inverted pendulum system

Control System Development

From the given mathematical modeling, the overall system could be converted into the block diagram representing the state-space model. In this model, the overall signal flowing could be shown clearly, and the input signal is consisted of two parts, the original step signal, which tests about how the system reacts to a constant input, and the band-limited white noise signal, which shows how the system reacts to constant and random disturbances. This open-loop control system, as discussed in the previous section, does not obtain a good stability and observability given a certain input signal, and it oscillates even when trivial disturbances is introduced. It can be shown from above that only a small disturbance is added to the 0-voltage input in the system, and oscillation occurs at the output. Applying the pole placement method, the desired poles in the complex plane are determined as follows: p_1 = -18+5i; p_2 = -18 - 5i; p_3 = -24; p_4 = -20, where $p_i, i = 1,2,3,4$ refers to the poles desired in the complex plane. In this case, by using the pole placement method for the controller, the state-feedback gain matrix K is obtained as follows:

$$K = \begin{bmatrix} -93.4536 \\ 24.1534 \\ -166.8072 \\ -34.5923 \end{bmatrix}$$

Similarly, we can have the observer designed for the new system, obtaining the observer matrix L. Having the desired poles for the observer listed below as: op_1=-10+5i, op_2=-10-5i; op_3=-15, op_4=-16. We use the same pole-polacement method and get the estimator gain which is :

$$L = \begin{bmatrix} 30.3264 & -5.4489 \\ 305.6514 & -40.6134 \\ 1.2864 & 25.9756 \\ -29.2065 & 256.6796 \end{bmatrix}$$

Thus by having the gain matrix K for controller and estimator gain matrix L, the new system, which is both observable and controllable, has a block-diagram shown as below:

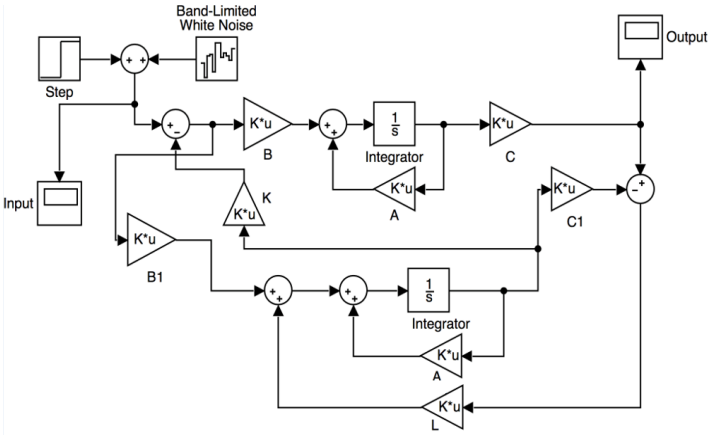

Figure 4. Simulink block-diagram for an observable and controllable system

In this case, after the controller and observer is introduced, we have the newly developed control system, and it can be seen that no phase-shift occured after the controller is introduced. Thus we may assume that the new system is under stable condition. Another analysis is done considering the step-response and impulse response of the system. The output plot for the step response is shown below as:

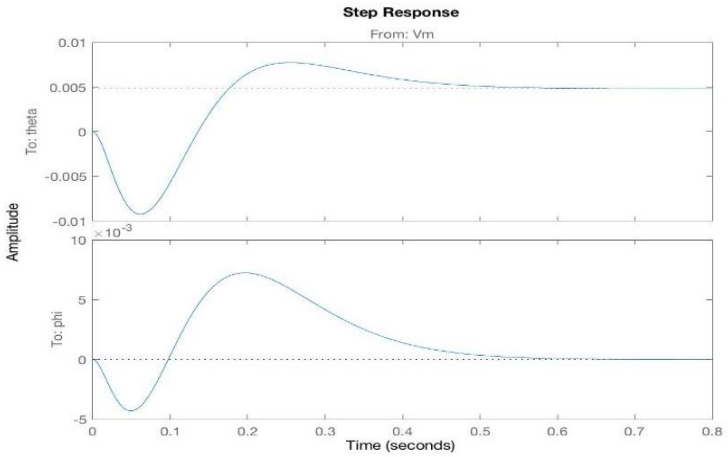

Figure 5. Step response of the closed loop system

Conclusion

In this paper, we had discussions on the rotary inverted pendulum, and simulation is done for the continuous system, which is the ideal case. Modeling of the original system is done with Euler-Lagrange Equations and linearization, and initial analysis of the open-loop system is done with the state-space method, indicating that without the controller, the system could not remain in a stable condition.

References

1 *T. C. Kuo, Y. J. Huang, and B. W. Hong, "Adaptive PID With Sliding Mode Control for The Rotary Inverted Pendulum System," IEEE/ASME International Conference on Advanced Intelligent Mechatronics, Vol. 3, pp. 1804–1809, 2009.*

2 K. Lai, Jin Xiao, Xiaoguang Hu, Jianxin Fan, Bing Wu, "Modeling and Control for Stability and Rotation Velocity of a Rotary Inverted Pendulum," 2015 IEEE 10th Conference on Industrial Electronics and Applications (ICIEA), 2015, pp. 955–960.

3 Y. Kim, S. H. Kim, and Y. K. Kwak, "Dynamic analysis of a nonholonomic two-wheeled inverted pendulum robot," Journal of Intelligent and Robotic Systems: Theory and Applications, Vol. 44, No. 1, 2005, pp. 25–46.

4 S. Awtar, C. Bernard, N. Boklund, A. Master, D. Ueda, and K. Craig, "Mechatronic design of a ball-on-plate balancing system," Mechatronics, Vol. 12, No. 2, 2002, pp. 217–228.

5 K. Furuta and H. Kajiwara, "Digital control of a double inverted pendulum on an inclined rail," International Journal of control, Vol. 7179, No. May 2012, 1980, pp. 37–41.

6 C. J. A. VanKats, "Nonlinear control of a Furuta Rotary inverted pendulum," Eindhoven University of Technology, June 2004.

7 A. M. Lopes, J. A. Tenreiro Machado, C. M. A. Pinto, and A. M. S. F. Galhano, "Fractional dynamics and MDS visualization of earthquake phenomena," Computers and Mathematics with Applications, Vol. 66, No. 5, 2013, pp. 647–658.

8 J. J. Wang, "Simulation studies of inverted pendulum based on PID controllers," Simulation Modelling Practice and Theory, Vol. 19, No. 1, 2011, pp. 440–449.

9 W. Liao, L. Zhengbo, S. Bi, and D. Wang, "Fractional PID based stability control for a single link rotary inverted pendulum," Proceedings of the 2015 International Conference on Advanced Mechatronic Systems, Beijing, China, August, 2015, pp. 22–24.

10 M. Akhtaruzzaman and a. a. Shafie, "Modeling and control of a rotary inverted pendulum using various methods, comparative assessment and result analysis," 2010 IEEE International Conference on Mechatronics and Automation, 2010, pp. 1342–1347.

11 H. Malek, Y. Luo, and Y. Chen, "Identification and tuning fractional order proportional integral controllers for time delayed systems with a fractional pole," Mechatronics, Vol. 23, No. 7, 2013, pp. 746–754.

12 J. Krishen and V. M. Becerra, "Efficient fuzzy control of a rotary inverted pendulum based on LQR mapping," IEEE International Symposium on Intelligent Control - Proceedings,2006, pp. 2701–2706.

13 E. Aranda-Escolástico, M. Guinaldo, M. Santos, and S. Dormido, "Control of a Chain Pendulum: A fuzzy logic approach," International Journal of Computational Intelligence Systems, Vol. 9, No. 2, 2016, pp. 281–295.

14 T. Takagi and M. Sugeno, "Fuzzy identification of systems and its applications to modeling and control," IEEE Transactions on Systems, Man and Cybernetics,, Vol. SMC-15, No. 1, 1985, pp. 116–132.

15 M. Park, Y. J. Kim, and J. J. Lee, "Swing-up and LQR stabilization of a rotary inverted pendulum," Artificial Life and Robotics, Vol. 16, No. 1, 2011, pp. 94–97.

16 R. El-Khazali, "Fractional-order PI $\lambda d\mu$ controller design," Computers and Mathematics with Applications, Vol. 66, No. 5, 2013, pp. 639–646.

17 I. Hassanzadeh and S. Mobayen, "Controller design for rotary inverted pendulum system using evolutionary algorithms," Mathematical Problems in Engineering, Vol. 2011, 2011, pp. 1-17. .

18 ——, "PSO-based controller design for rotary inverted pendulum system," Journal of Applied Sciences, Vol. 8, No. 16, 2008, pp. 2907–2912.

19 V. Sukontanakarn and M. Parnichkun, "Real-time optimal control for rotary inverted pendulum," American Journal of Applied Sciences, Vol. 6, No. 6, 2009, pp. 1106–1115.

20 N. Muskinja and B. Tovornik, "Swinging up and stabilization of a real inverted pendulum," IEEE Transactions on Industrial Electronics, Vol. 53, No. 2, 2006, pp. 631–639.

21 T. K. Chye, "Rotary Inverted Pendulum Teo Chun Sang School of Electrical and Electronic Engineering Nanyang Technological University," Rotary Inverted Pendulum Teo Chun Sang School of Electrical and Electronic Engineering, Nanyang Technological University, 1998.

22 M. Roman, E. Bobasu, and D. Sendrescu, "Modelling of the rotary inverted pendulum system," 2008 IEEE International Conference on Automation, Quality and Testing, Robotics, AQTR 2008 - THETA 16th Edition - Proceedings, Vol. 2, 2008, pp. 141–146.

23 X. Diao, "Rotary Inverted Pendulum," New Mexico State University, July 2006.

24 T. N. L. Vu and M. Lee, "Analytical design of fractional-order proportional-integral controllers for time-delay processes," ISA Transactions, Vol. 52, No. 5, 2013, pp. 583–591.

25 S. Jadlovská and J. Sarnovský, "Modelling of classical and rotary inverted pendulum systems - A generalized approach," Journal of Electrical Engineering, Vol. 64, No. 1, 2013, pp. 12–19.

26 *E. d. C. Gomes, L. A. de S. Ribeiro, J. V. M. Caracas, S. Y. C. Catunda, and R. D. Lorenz, "State space decoupling control design methodology for switching converters," 2010 IEEE Energy Conversion Congress and Exposition, 2010, pp. 4151–4158.*

Wangling Yu

Is an assistant professor in the Electrical & Computer Engineering Technology Department of the Purdue University Northwest. He was a test engineer over 15 years, providing technical leadership in the certification, testing and evaluation of custom integrated security systems. He received his PhD degree in Electrical Engineering from the City University of New York in 1992, specializing in control theory and electronic technology.

Hanlin Chen

Received MS in Mechanical Engineering Technology at Purdue University in 2016. Currently, she is a PhD student in Computer Information Technology at Purdue University.

Digital Controller Design for Mechatronic Rotary Inverted Pendulum (Part 2)

Hanlin Chen[1] and Wangling Yu[2]

1 Polytechnic Institute, Purdue University, West Lafayette, IN 47907
2 College of Technology, Purdue University Northwest, Westville, IN 46391

Abstract

The mechatronic rotary inverted pendulum is a fourth order dynamic system. The digital control of PID, LQR, and pole placement are investigated, and a controller is designed by doing zero-pole analysis, root-locus analysis, and Nyquist diagram. Various methods on the design of the controller are also applied, including PID, LQR, pole placement and so on.

Keywords

Pole placement, rotary inverted pendulum, digital control stability

Introduction

This paper is a continuation of Part 1 analog controller design for the mechatronic rotary inverted pendulum, which is a typical fourth order nonlinear dynamic system. The mathematical model of rotary inverted pendulum system has been derived, and its analog controller design can function as a reference and a comparison to the digital controller design for this system. LQR and pole placement are special cases of eigenstructure assignment, because the eigenstructure assignment problem of rotary inverted pendulum actually is to assign both the eigenvalues and their corresponding eigenvectors for this system control[1]. The digital control of PID, LQR, and pole placement are investigated. Simulink simulations are given to justify the theoretical analysis for the control approach and its effect verification.

Modeling of Rotary Inverted Pendulum [2]

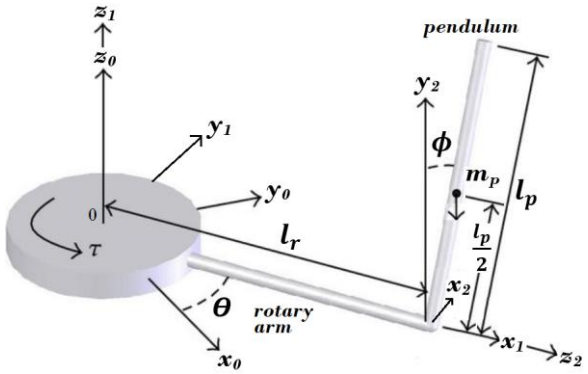

Figure 1. Rotary inverted pendulum and its coordinate systems[2]

As shown in Figure 1, The Lagrange function L expresses the conversion between kinematic energy and potential energy. Using the Euler-Lagrange equation, the dynamics of the rotary inverted pendulum can be derived as:

$$\left(J_r + m_p l_r^2\right)\ddot{\theta} - \frac{1}{2}m_p l_r l_p \ddot{\phi} cos\phi + \frac{1}{2}m_p l_r l_p \dot{\phi}^2 sin\phi = \tau \tag{1}$$

$$\left(J_p + \frac{1}{4}m_p l_p^2\right)\ddot{\phi} - \frac{1}{2}m_p l_r l_p \ddot{\theta} cos\phi - \frac{1}{2}m_p l_r l_p \dot{\theta}\dot{\phi} sin\phi = 0 \tag{2}$$

And its state space expression is as follows:

$$\begin{bmatrix} \dot{\theta} \\ \ddot{\theta} \\ \dot{\phi} \\ \ddot{\phi} \end{bmatrix} = \begin{bmatrix} 0 & 1 & 0 & 0 \\ 0 & \frac{(c_3 * K_T * K_m)}{(R_m * (c_1 * c_3 - c_2 * c_4)} & \frac{c_2 * c_5}{c_1 * c_3 - c_2 * c_4} & 0 \\ 0 & 0 & 0 & 1 \\ 0 & \frac{c_4 * K_T * K_m}{R_m * (c_1 * c_3 - c_2 * c_4)} & -\frac{c_5}{c_3} & 0 \end{bmatrix} \begin{bmatrix} \theta \\ \dot{x}\theta \\ \phi \\ \dot{\phi} \end{bmatrix} + \begin{bmatrix} 0 \\ \frac{c_3 * K_T}{R_m * (c_1 * c_3 - c_2 * c_4)} \\ 0 \\ -\frac{c_4 * K_T}{R_m * (c_1 * c_3 - c_2 * c_4)} \end{bmatrix} u \tag{3}$$

$$y = \begin{bmatrix} 1 & 0 & 0 & 0 \\ 0 & 0 & 1 & 0 \end{bmatrix} \begin{bmatrix} \theta \\ \dot{\theta} \\ \phi \\ \dot{\phi} \end{bmatrix} + \begin{bmatrix} 0 \\ 0 \end{bmatrix} u \tag{4}$$

Given a group of parameters, this mathematical model can be used for numerical simulation.

Digital Control

Given the condition of the system that the digital control should take place rather than continuous-time controlling, after the configuration of the system modelling as the continuous-time model, the converting process from continuous-time to discrete-time would take place.

When considering the discrete-time control system, it should be noted that a trade-off between the sampling accracy and the sampling cost should be considered. Generally speaking, the higher the sampling frequency is, the lower the possibility that aliasing occures, while also the cost of the sampling increases and the upper-bound of it exists due to the condition of the actual hardward. In this case given the condition that we need to have the pendulum maintain a constant stable status, thus we assume that the input signal has a period of $T = 1$. And to make evaluation easier, the sampling frequency of digital system is set to be $f = 20Hz$.

Having a sampling time as $T = 0.05s$, we convert the model representation from continuous model to discrete model using the ZOH method, and it reveals the following representation:

The transfer matrix for the model itself is shown below as:

$$G = \begin{bmatrix} 1 & 0 & 0 & 0 & 0 \\ 0 & 1 & 0 & 0 & 0 \\ 0 & 0 & 1 & 0 & 0 \\ 0 & 0 & 0 & 1 & 0 \end{bmatrix}$$

With the transfer matrix shown above, we have the discrete model for the rotary inverted pendulum with state-space representation below:

$$A_d = U_1 * \Sigma_1 * V_1$$

where U_1 and V_1 are 8x8 unitary matrices. Accordingly, Σ_1 is a diagonal matrix with eigenvalue 156.7777, 21.5955, 5.6460, 1.2824, 0.8070, 0.0533. Similarly, as discussed in the section. the decoupling process can be excuted after the SVD decomposition of matrix A_d, and given the variables involved in the system has 8 variables listed as $\theta, \hat{\theta}, \dot{\theta}, \dot{\hat{\theta}}, \phi, \hat{\phi}, \dot{\phi}, \dot{\hat{\phi}}$. So accordingly, the relationships between the variables are listed below as:

$$\dot{\theta} = U_{1,:} * \sigma_1 * V_{:,1} * \theta + B_1 u$$

$$\dot{\hat{\theta}} = U_{2,:} * \sigma_2 * V_{:,2} * \hat{\theta} + B_2 u$$

$$\ddot{\theta} = U_{3,:} * \sigma_3 * V_{:,3} * \dot{\theta} + B_3 u$$

$$\ddot{\hat{\theta}} = U_{4,:} * \sigma_4 * V_{:,4} * \dot{\hat{\theta}} + B_4 u$$

$$\dot{\phi} = U_{5,:} * \sigma_5 * V_{:,5} * \phi + B_5 u$$

$$\dot{\hat{\phi}} = U_{6,:} * \sigma_6 * V_{:,6} * \hat{\phi} + B_6 u$$

$$\ddot{\phi} = U_{7,:} * \sigma_7 * V_{:,7} * \dot{\phi} + B_7 u$$

$$\ddot{\hat{\phi}} = U_{8,:} * \sigma_8 * V_{:,8} * \dot{\hat{\phi}} + B_8 u$$

By substituing the numerical values into the equations shown above, the relations for the decoupled system reveals as:

$$\dot{\theta} = 103.1457 * \theta + B_1 u$$

$$\dot{\hat{\theta}} = -7.6926 * \hat{\theta} + B_2 u$$

$$\ddot{\theta} = -1.8416 * \dot{\theta} + B_3 u$$

$$\ddot{\hat{\theta}} = 0.2517 * \dot{\hat{\theta}} + B_4 u$$

$$\dot{\phi} = -0.0721 * \phi + B_5 u$$

$$\dot{\hat{\phi}} = 0.0011 * \hat{\phi} + B_6 u$$

$$\ddot{\phi} = 5.5892 * 10^{-4} * \dot{\phi} + B_7 u$$

$$\ddot{\hat{\phi}} = 5.3242 * 10^{-5} * \dot{\hat{\phi}} + B_8 u$$

To verify the controlability of the desretized system, we plot the zero-pole of the digital controlled system, which is shown below as:

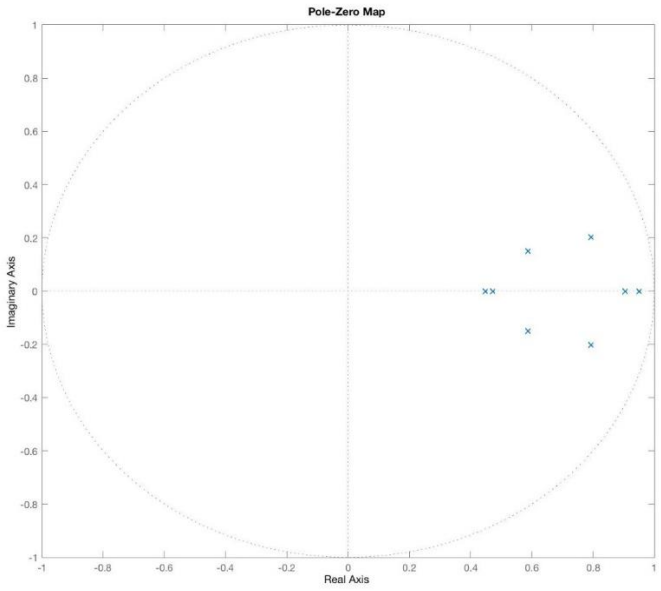

Figure 2. Zero-pole of the digital controlled system

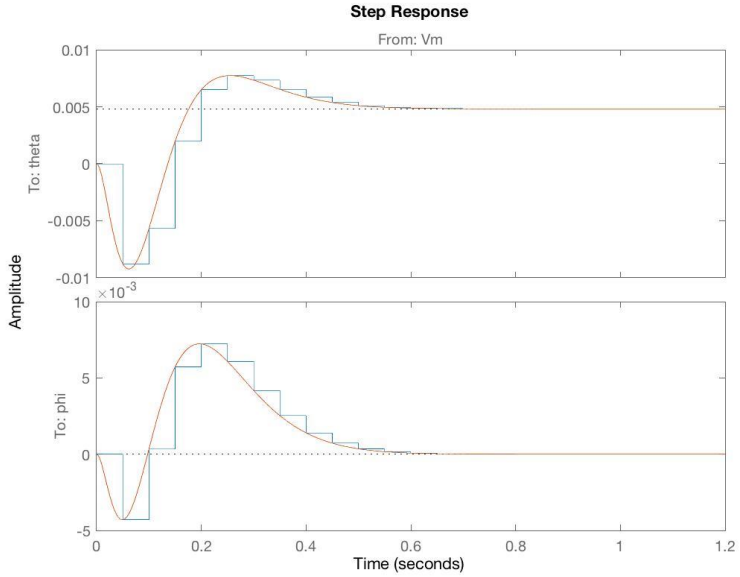

Figure 3. Step response of the digital controlled system

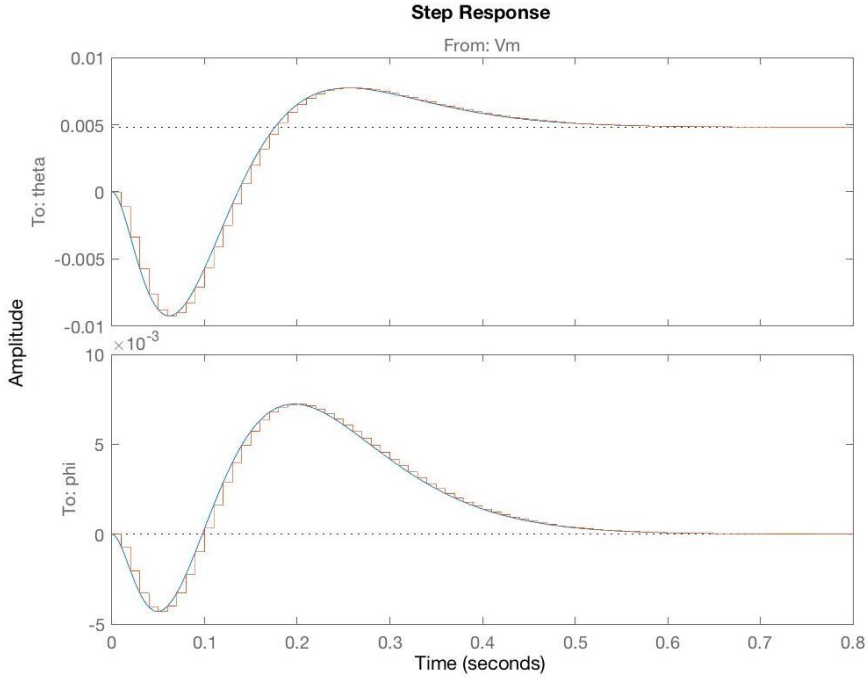

Figure 4. Step response of closed loop system with 100 Hz sampling rate

Noticing the fact that both zeros and poles of the controled system lies within the unit circle of the complex plane, it is verified that the digital system which controller is applied is stable, yet with more errors due to a lower sampling rate. Such error could be fixed by increasing the samplign rate or decreasing the sampling time. For example, increasing the sampling time from *20Hz* to *100Hz*, the error between descrete system and continuous system decreased as shown below. Noticing the fact that although the sampling rate of *20Hz* seemed able to work, when it comes to

actual application such sampling rate for the comtroller is too low to get the pendulum in a stable condition, since the error could not be niglected, thus by comparing the two step response of the digital contollers and their related errors, the sampling rate of *100Hz* seemed more acceptable.

Conclusion

In this paper, we had discussions on the rotary inverted pendulum, and simulation is done for the discrete-control system, which can be applied with digital system. Modeling of the original system is done with Euler-Lagrange Equations and linearization, and initial analysis of the open-loop system is done with the state-space method, indicating that without the controller, the system could not remain in a stable condition. The controller design method for the descrete control system is that the controller for the continuous system is first designed, and then the continuous-descrete conversion is done using ZOH method. Such method enables both the controlability and the obserbility for the descrete system. To decrease the sampling error, the sampling rate should be increased, yet the hardware condition of the digital controller also restricts the upper bound of the sampling rate.

References

1 *Jiafan Zhang, Huajiang Ouyang, and Jun Yang, "Partial Eigenstructure assignment for undamped vibration systems using acceleration and displacement feedback," Journal of Sound and Vibration, Vol. 333, No. 1, 2014, pp. 1-12.*

2 *Wangling Yu, and Hanlin Chen, "*Analog Controller Design for Mechatronic Rotary Inverted Pendulum (Part 1)", ASEE Mid-Atlantic Conference Section Spring Conference, Washington, April 6-7, 2018.

Hanlin Chen

Received MS in Mechanical Engineering Technology at Purdue University in 2016. Currently, she is a PhD student in Computer Information Technology at Purdue University.

Wangling Yu

Is an assistant professor in the Electrical & Computer Engineering Technology Department of the Purdue University Northwest. He was a test engineer over 15 years, providing technical leadership in the certification, testing and evaluation of custom integrated security systems. He received his PhD degree in Electrical Engineering from the City University of New York in 1992, specializing in control theory and electronic technology.